J|A|C|S ARTICLES

Published on Web 02/16/2009

One- and Two-Electron Reactivity of a Tantalum(V) Complex with a Redox-Active Tris(amido) Ligand

Andy I. Nguyen, Karen J. Blackmore, Shawn M. Carter, Ryan A. Zarkesh, and Alan F. Heyduk*

Department of Chemistry, University of California, Irvine, California 92697

Received October 30, 2008; E-mail: aheyduk@uci.edu

Abstract: A new redox-active, tris(amido) ligand platform, bis(2-isopropylamino-4-methoxyphenylamine $[NNN^{cat}]^{3-}$, has been prepared and used in the preparation of tantalum(V) complexes. The ligand was prepared in its protonated form by a three-step procedure from commercially available 4-methoxy-2-nitroaniline and 1-iodo-4-methoxy-2-nitrobenzene. Direct reaction of $[NNN^{cat}]H_3$ with $TaCl_2Me_3$ afforded five-coordinate $[NNN^{cat}]TaCl_2$ (**1**), which accepted the strong σ-donor ligand ^{t}BuNC to form the six-coordinate adduct $[NNN^{cat}]TaCl_2(CN^tBu)$ (**2**). Complex **1** is formally a d^0, Ta^V complex; however, one- and two-electron reactivity is enabled at the metal center by the redox-activity of the ligand platform. Complex **1** was oxidized by one electron to afford the radical species $[NNN^{sq\bullet}]TaCl_3$ (**3**), which was characterized by solution EPR spectroscopy. Cyclic voltammetry studies of complex **3** showed clean one-electron oxidation and reduction processes at 0.148 and -0.324 V vs $[Cp_2Fe]^{+/0}$, indicating the accessibility of three oxidation states, $[NNN^{cat}]^{3-}$, $[NNN^{sq\bullet}]^{2-}$, and $[NNN^{q}]^{-}$, for the metallated ligand. Complex **1** also can undergo two-electron reactions, as evidenced by the reaction with nitrene transfer reagents to form tantalum imido species. Thus **1** reacted with organic azides, RN_3 (R = Ph, *p*-C_6H_4Me, *p*-$C_6H_4{}^tBu$), to form $[NNN^q]TaCl_2(=NR)$ (**4**). Similarly, the tantalum diphenylmethylidenehydrazido complex, $[NNN^q]TaCl_2(=NNCPh_2)$ (**5**), was formed by reaction of **1** with the diazoalkane, N_2CPh_2.

Introduction

Synthetic transition-metal imido complexes continue to be of interest both for their interesting stereoelectronic properties and for their potential application as new nitrene transfer catalysts. Methods for preparing these species include nonredox mechanisms, such as the deprotonation of coordinated amino and amido ligands, alkylation of metal nitrides, and oxo/imido metathesis reactions, which are suitable for virtually any type of transition metal complex.[1] Redox mechanisms for preparing imido complexes, including the reactions of metal complexes with organic azides[2] and organic diazo complexes,[3] require that the metal center, M^{n+}, be oxidized by two electrons to a stable $M^{(n+2)+}$ oxidation state (in the cases in which the imido ligand bridges two metal centers, each metal center must have an accessible $M^{(n+1)+}$ oxidation state).[4] This type of mechanism is equivalent in many ways to an oxidative addition reaction; in this case, a neutral nitrene fragment is transferred to the metal, resulting in a formal two-electron oxidation of the metal center and the formation of two new metal−nitrogen bonds. This oxidative pathway to metal imido complexes has recently been exploited for the synthesis of a variety of mid- and late-transition metal imido species with implications for catalysis if the nitrene could be transferred selectively to a hydrocarbon substrate.

Our research efforts focus on the development of multielectron redox reactivity for electrophilic early transition metal complexes, specifically those with formal d^0 valence electron counts at the metal.[5] Catecholates and related ligands provide a mechanism for introducing redox properties to d^0 metal complexes through ligand-based redox activity. One-electron oxidation of a catecholate affords the semiquinonate; a second one-electron oxidation affords the quinone form of the ligand.[6] The spectroscopic and electrochemical properties of metal

(1) (a) Nugent, W. A.; Haymore, B. L. *Coord. Chem. Rev.* **1980**, *31*, 123–175. (b) Nugent, W. A.; Mayer, J. M. *Metal-Ligand Multiple Bonds*; John Wiley and Sons: New York, 1988. (c) Wigley, D. E. *Prog. Inorg. Chem.* **1994**, *42*, 239–482.

(2) (a) Waterman, R.; Hillhouse, G. L. *J. Am. Chem. Soc.* **2008**, *130*, 12628–12629. (b) Bart, S. C.; Lobkovsky, E.; Bill, E.; Chirik, P. J. *J. Am. Chem. Soc.* **2006**, *128*, 5302–5303. (c) Abu-Omar, M. M.; Shields, C. E.; Edwards, N. Y.; Eikey, R. A. *Angew. Chem., Int. Ed.* **2005**, *44*, 6203–6207. (d) Kogut, E.; Wiencko, H. L.; Zhang, L.; Cordeau, D. E.; Warren, T. H. *J. Am. Chem. Soc.* **2005**, *127*, 11248–11249. (e) Hu, X.; Meyer, K. *J. Am. Chem. Soc.* **2004**, *126*, 16322–16323. (f) Brown, S. D.; Betley, T. A.; Peters, J. C. *J. Am. Chem. Soc.* **2003**, *125*, 322–323. (g) Thyagarajan, S.; Shay, D. T.; Incarvito, C. D.; Rheingold, A. L.; Theopold, K. H. *J. Am. Chem. Soc.* **2003**, *125*, 4440–4441. (h) Jenkins, D. M.; Betley, T. A.; Peters, J. C. *J. Am. Chem. Soc.* **2002**, *124*, 11238–11239.

(3) (a) Tsai, Y.-C.; Wang, P.-Y.; Lin, K.-M.; Chen, S.-A.; Chen, J.-M. *Chem. Comm.* **2008**, 205–207. (b) Evans, W. J.; Miller, K. A.; Kozimor, S. A.; Ziller, J. W.; DiPasquale, A. G.; Rheingold, A. L. *Organometallics* **2007**, *26*, 3568–3576. (c) Kilgore, U. J.; Yang, X.; Tomaszewski, J.; Huffman, J. C.; Mindiola, D. J. *Inorg. Chem.* **2006**, *45*, 10712–10721. (d) Lentz, M. R.; Vilardo, J. S.; Lockwood, M. A.; Fanwick, P. E.; Rothwell, I. P. *Organometallics* **2004**, *23*, 329–343.

(4) Badiei, Y. M.; Krishnaswamy, A.; Melzer, M. M.; Warren, T. H. *J. Am. Chem. Soc.* **2006**, *128*, 15056–15057.

(5) Ketterer, N. A.; Fan, H.; Blackmore, K. J.; Yang, X.; Ziller, J. W.; Baik, M.-H.; Heyduk, A. F. *J. Am. Chem. Soc.* **2008**, *130*, 4364–4374.

(6) (a) Pierpont, C. G *Coord. Chem. Rev.* **2001**, *219−221*, 415–433. (b) Pierpont, C. G.; Lange, C. W. *Prog. Inorg. Chem.* **1994**, *41*, 331–443. (c) Pierpont, C. G.; Buchanan, R. M. *Coord. Chem. Rev.* **1981**, *38*, 45–87.

complexes with catecholate-derived ligands have received considerable attention,[7] and a clearer picture on the assignment of metal- and ligand-based redox processes has developed.[8] The utilization of such ligand-based redox properties for chemical transformations at the metal center has been more limited. Our group has utilized amidophenolate ligands to enable oxidative addition[9] and reductive elimination[10] reactions to d^0, zirconium(IV) complexes. More recently, we have harnessed the redox-activity of a tridentate amidophenolate ligand to enable the four-electron oxidative formation of aryldiazenes in a tantalum(V) dimer.[11] Other multielectron reactions that rely on ligand-based redox, which have been reported recently include the addition of O_2 to a zirconium(IV) complex,[12] the coordination of N_2 to an Fe(II) complex,[13] and the catalytic oxidation of H_2 by an iridium complex.[14]

This manuscript reports the tantalum coordination chemistry of a new tridentate redox-active ligand. Bis(2-isopropylamino-4-methoxyphenyl)amine ($[NNN^{cat}]H_3$) was prepared by a three-step procedure starting from 4-methoxy-2-nitroaniline and 1-iodo-4-methoxy-2-nitrobenzene. As shown in Chart 1, when $[NNN^{cat}]^{3-}$ is coordinated to tantalum, it can be oxidized by one electron to afford the radical semiquinone form, $[NNN^{sq\bullet}]^{2-}$, and by a second electron to afford the quinone form, $[NNN^{q}]^{-}$. The tantalum complexes of $[NNN^{cat}]^{3-}$ and $[NNN^{sq\bullet}]^{2-}$ show spectroscopic signatures consistent with delocalization of the ligand valence electron density onto the metal, suggesting noninnocent electronic behavior. Furthermore, this mixing of ligand and metal valence electrons enables one- and two-electron oxidative-addition reactivity to occur at a formal d^0, tantalum(V) center, exemplified by the transfer of a nitrene from an organic azide to $[NNN^{cat}]TaCl_2$ to form a tantalum imide complex, $[NNN^{q}]Ta(=NPh)Cl_2$.

Experimental Section

Synthetic Considerations. The complexes described below are air- and moisture-sensitive. All manipulations were carried out under an atmosphere of argon or nitrogen gas using standard Schlenk, vacuum-line, and glovebox techniques. High-purity solvents initially were sparged with argon and then passed through activated alumina and Q5 columns to remove water and oxygen, respectively. The reagents 4-methoxy-2-nitroaniline, 1-iodo-4-methoxy-2-nitrobenzene, *tert*-butylisocyanide, and $[Cp_2Co][PF_6]$ were used as received. Dichloroiodobenzene,[15] aryl azides,[16] diphenyldiazomethane,[17] and $TaMe_3Cl_2$[18] were prepared according to published procedures. The electrolyte $[^nBu_4N][PF_6]$ was recrystallized three times from hot methanol and dried under high vacuum.

Chart 1

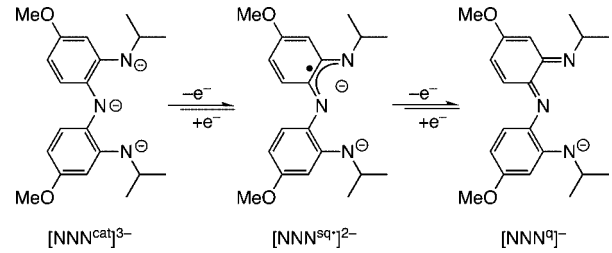

Physical Methods. All complexes were characterized by ^1H and ^{13}C NMR spectroscopy, IR spectroscopy, and elemental analysis. NMR spectra were collected on Bruker Avance 500 or 600 MHz spectrometers in either $CDCl_3$ or C_6D_6 solvents that were degassed by several freeze−pump−thaw cycles, dried over sodium benzophenone-ketyl radical, and vacuum-distilled before use. ^1H and ^{13}C NMR spectra were referenced to TMS using the residual ^1H and natural abundance ^{13}C impurities of the solvent. All chemical shift values are reported using the standard δ notation in ppm. Infrared spectra (450−4000 cm^{-1}) were recorded on a Perkin-Elmer Spectrum One spectrophotometer as KBr pellets. UV−vis absorbance spectra (270−900 nm) were recorded on a Perkin-Elmer Lambda 800 double-beam spectrophotometer equipped with a PMT detector. EPR spectra were collected on a Bruker EMX X-band spectrometer equipped with an ER041XG microwave bridge. Spectra for EPR samples were collected using the following spectrometer settings: attenuation = 25 dB, microwave power = 0.639 mW, frequency = 9.09 GHz, sweep width = 3000 G, modulation amplitude = 9.02 G, gain = 5.02×10^3, conversion time = 20.48 ms, time constant = 163.84 ms, and resolution = 2048 points. Electrochemical measurements were recorded with a Gamry G300 potentiostat using an electrochemical cell comprising a 1.5 mm diameter platinum disk electrode, a silver wire reference electrode, and a platinum wire auxiliary electrode. Cyclic voltammograms were recorded in a glovebox at room temperature in CH_2Cl_2 solution containing 0.1 M $[^nBu_4N][PF_6]$ as the supporting electrolyte. All potentials were referenced to $[Cp_2Fe]^{+/0}$ using an internal $[Cp_2Co]^{+/0}$ standard ($E^{o\prime} = -1.336$ V vs $[Cp_2Fe]^{+/0}$).[19] Under our conditions the typical solvent window is from a reductive limit of −1.20 V to an oxidative limit of 1.77 V. Schwarzkopf Microanalytical Laboratory provided elemental analyses.

Preparation of Bis(4-methoxy-2-nitrophenyl)amine. A round-bottomed flask, equipped with a stir bar and reflux condenser, was charged with 4-methoxy-2-nitroaniline (9.00 g, 53.5 mmol, 1 equiv), 1-iodo-4-methoxy-2-nitrobenzene (15.0 g, 53.7 mmol, 1 equiv), copper powder (1.75 g, 27.5 mmol, 0.5 equiv), and potassium carbonate (5.00 g, 36.2 mmol, 0.7 equiv). The reaction mixture was heated to a melt for 1 h. Once the melt had thickened, toluene (15 mL) was added and the mixture was allowed to reflux for 4 h. The product was isolated by Soxhlet extraction using toluene (100 mL) for 2 days. The dark-red needles were collected by filtration (6.80 g, 40%). ^1H NMR (500 MHz, $CDCl_3$) δ 3.86 (*s*, 6H, OCH_3), 7.13 (dd, 2H, aryl-H, $^3J_{HH} = 9.1$, $^4J_{HH} = 3.0$), 7.38 (d, 2H, aryl-H, $^3J_{HH} = 9.1$), 7.65 (d, 2H, aryl-H, $^4J_{HH} = 3.0$), 10.61 (s, 1H, NH). ^{13}C NMR (125.8 MHz, $CDCl_3$) δ 55.9 (OCH_3), 108.5 (aryl-C), 121.3 (aryl-C), 123.8 (aryl-C), 131.83 (aryl-C), 138.4 (aryl-C), 153.8 (aryl-C).

Preparation of Bis(2-amino-4-methoxyphenyl)amine. Powdered zinc (17 g, 260 mmol, 19 equiv) was added quickly to a

(7) (a) Ray, K.; Petrenko, T.; Wieghardt, K.; Neese, F. *Dalton Trans.* **2007**, 1552–1566. (b) Ward, M. D.; McCleverty, J. A. *J. Chem. Soc., Dalton Trans.* **2002**, 275–288. (c) Pierpont, C. G.; Lange, C. W. *Prog. Inorg. Chem.* **1994**, *41*, 331–443.
(8) (a) Chaudhuri, P.; Verani, C. N.; Bill, E.; Bothe, E.; Weyhermüller, T.; Wieghardt, K. *J. Am. Chem. Soc.* **2001**, *123*, 2213–2223. (b) Chun, H.; Verani, C. N.; Chaudhuri, P.; Bothe, E.; Bill, E.; Weyhermüller, T.; Wieghardt, K. *Inorg. Chem.* **2001**, *40*, 4157–4166.
(9) (a) Blackmore, K. J.; Ziller, J. W.; Heyduk, A. F. *Inorg. Chem.* **2005**, *44*, 5559–5561. (b) Blackmore, K. J.; Sly, M. B.; Haneline, M. R.; Ziller, J. W.; Heyduk, A. F. *Inorg. Chem.* **2008**, *47*, in press.
(10) Haneline, M. R.; Heyduk, A. F. *J. Am. Chem. Soc.* **2006**, *128*, 8410–8411.
(11) Zarkesh, R. A.; Ziller, Z. W.; Heyduk, A. F. *Angew. Chem., Int. Ed.* **2008**, *47*, 4715–4718.
(12) Stanciu, C.; Jones, M. E.; Fanwick, P. E.; Abu-Omar, M. M. *J. Am. Chem. Soc.* **2007**, *129*, 12400–12401.
(13) Bart, S. C.; Chłopek, K.; Bill, E.; Bouwkamp, M. W.; Lobkovsky, E. B.; Neese, F.; Wieghardt, K.; Chirik, P. J. *J. Am. Chem. Soc.* **2006**, *128*, 13901–13912.
(14) Ringenberg, M. R.; Kokatam, S. L.; Heiden, Z. M.; Rauchfuss, T. B. *J. Am. Chem. Soc.* **2008**, *130*, 788–789.
(15) Lucas, H. J.; Kennedy, E. R. *Org. Synth.* **1942**, *22*, 69–70.
(16) (a) Smith, P. A. S.; Brown, B. B. *J. Am. Chem. Soc.* **1951**, *73*, 2438–2441. (b) Barral, K.; Moorhouse, A. D.; Moses, J. E. *Org. Lett.* **2007**, *9*, 1809–1811.
(17) Smith, L. I.; Howard, K. L. *Org. Synth.* **1944**, *24*, 53–54.
(18) Schrock, R. R.; Sharp, P. R. *J. Am. Chem. Soc.* **1978**, *100*, 2389–2399.
(19) Connelly, N. G.; Geiger, W. E. *Chem. Rev.* **1996**, *96*, 877–910.

slurry of bis(4-methoxy-2-nitrophenyl)amine (4.30 g, 13.4 mmol, 1 equiv) in glacial acetic acid (130 mL). The reaction mixture was stirred at room temperature overnight under a slow purge of argon during which time the color changed to pale yellow. The solution was filtered and added to a 1 M aqueous solution of sodium dithionite (600 mL). Concentrated ammonium hydroxide (200 mL) was added slowly to the filtrate resulting in the precipitation of a white solid. The product was collected by gravity filtration and washed with water (2.25 g, 65%). ^{1}H NMR (600 MHz, $CDCl_3$) δ 3.74 (broad, 5H, NH), 3.74 (s, 6H, OCH_3), 6.28 (dd, 2H, aryl-H, $^4J_{HH} = 2.7$, $^3J_{HH} = 8.5$), 6.37 (d, 2H, aryl-H, $^4J_{HH} = 2.7$), 6.61 (d, 2H, aryl-H, $^3J_{HH} = 8.5$). ^{13}C NMR (125.8 MHz, $CDCl_3$) δ 55.4 (OCH_3), 102.6 (aryl-C), 104.1 (aryl-C), 121.5 (aryl-C), 125.2 (aryl-C), 139.8 (aryl-C), 156.3 (aryl-C).

Preparation of Bis(2-isopropylamino-4-methoxyphenyl)amine ([NNN^{cat}]H$_3$). Under argon, a three-neck round-bottom flask, equipped with a gas inlet, rubber septum, and a solid-addition flask containing sodium cyanoborohydride (2.25 g, 35.8 mmol, 4 equiv), was charged with bis(2-amino-4-methoxyphenyl)amine (2.25 g, 8.7 mmol, 1 equiv) and a degassed solution of methanol (45 mL), acetone (1.2 mL), and concentrated hydrochloric acid (1.4 mL). Once the solution became homogeneous, the solid sodium cyanoborohydride was added. The solution was stirred overnight until it turned yellow and then the volatiles were removed under reduced pressure. The residue was transferred to an argon-filled glovebag, dissolved in dichloromethane (300 mL), and washed with aqueous sodium dithionite and sodium bicarbonate solutions (1 M, 200 mL). The aqueous layers were extracted with additional dichloromethane (2 × 300 mL), and the combined organic layers were dried over magnesium sulfate and concentrated under reduced pressure to afford the product as an orange oil. This crude oil was purified by Kugelrohr distillation (0.2 mTorr, 160 °C) to give the product as a viscous, yellow-orange oil (1.86 g, 62%). ^{1}H NMR (500 MHz, C_6D_6) δ 0.93 (d, 12H, $^3J_{HH} = 6.3$, $CH(CH_3)_2$), 3.83 (sept, 2H, $^3J_{HH} = 6.3$, $CH(CH_3)_2$), 3.45 (*s*, 6H, OCH_3), 3.81 (s, 2H, NH), 4.05 (*s*, 1H, NH), 6.20 (dd, 2H, $^3J_{HH} = 8.4$, $^4J_{HH} = 2.7$, aryl-H), 6.49 (d, 2H, $^4J_{HH} = 2.7$, aryl-H), 6.67 (d, 2H, $^3J_{HH} = 8.4$, aryl-H). ^{13}C NMR (125.8 MHz, C_6D_6) δ 22.9 ($CH(CH_3)_2$), 44.1 ($CH(CH_3)_2$), 54.9 (OCH_3), 99.8 (aryl-C), 100.7 (aryl-C), 122.2 (aryl-C), 125.6 (aryl-C), 142.0 (aryl-C), 157.8 (aryl-C).

Preparation of [NNN^{cat}]TaCl$_2$ (1). A solution of [NNN^{cat}]H$_3$ (1.35 g, 3.9 mmol, 1 equiv) in diethyl ether (20 mL) was chilled to −35 °C and added slowly to a round-bottomed flask containing a cold solution of trimethyltantalum dichloride (1.17 g, 3.9 mmol, 1 equiv) in diethyl ether (20 mL). The reaction was allowed to warm to room temperature and was stirred overnight. Volatiles were removed under reduced pressure and the residue was washed with cold cyclopentane (3 × 10 mL) to afford a brick red solid (2.10 g, 90%). X-ray quality crystals were obtained from chilled, saturated cyclopentane solutions of the complex. Anal. Calcd for $C_{20}H_{26}Cl_2N_3O_2Ta$: C, 40.56; H, 4.42; N, 7.09. Found: C, 40.34; H, 4.89; N, 7.03. ^{1}H NMR (500 MHz, C_6D_6) δ 1.35 (d, 12H, $^3JHH =$ 6.5, $CH(CH_3)_2$), 3.43 (s, 6H, OCH_3), 4.54 (sept, 2H, $^3J_{HH} = 6.5$, $CH(CH_3)_2$), 6.24 (dd, 2H, $^3J_{HH} = 8.9$, $^4J_{HH} = 2.3$, aryl-H), 6.42 (d, 2H, $^4J_{HH} = 2.3$, aryl-H), 7.37 (d, 2H, $^3J_{HH} = 8.9$, aryl-H). ^{13}C NMR (125.8 MHz, C_6D_6) δ 16.9 ($CH(CH_3)_2$), 47.5 ($CH(CH_3)_2$), 54.9 (OCH_3), 92.6 (aryl-C), 99.4 (aryl-C), 105.2 (aryl-C), 113.7 (aryl-C), 142.0 (aryl-C), 146.7 (aryl-C). IR (KBr) $\bar{\nu}$/cm^{-1}: 2967, 2928, 1572, 1459, 1262, 1229, 1166, 1105, 1026, 823, 790, 650, 567, 524. UV−vis (toluene) λ_{max}/nm (ε/M^{-1} cm^{-1}): 311 (14 353).

Preparation of [NNN^{cat}]TaCl$_2$(CN^{t}Bu) (2). A solution of **1** (0.100 g, 0.17 mmol, 1 equiv) in toluene (10 mL) was treated with *tert*-butyl isocyanide (0.019 g, 0.23 mmol, 1.3 equiv). The solution was stirred overnight at room temperature. Volatiles were removed under reduced pressure leaving the product as a red-purple solid that was washed with cyclopentane (3 × 10 mL) (0.11 g, 92%). ^{1}H NMR (500 MHz, C_6D_6) δ 0.59 (s, 9H, $C(CH_3)_3$), 1.45 (s, br, 12H, $CH(CH_3)_2$), 3.38 (s, 6H, OCH_3), 5.57 (m, 2H, $CH(CH_3)_2$), 6.20 (dd, 2H, $^3J_{HH} = 8.9$, $^4J_{HH} = 2.6$, aryl-H), 6.40 (d, 2H, $^4J_{HH} =$ 2.6, aryl-H), 7.27 (d, 2H, $^3J_{HH} = 8.9$, aryl-H). ^{13}C NMR (125.8 MHz, C_6D_6) δ 16.9 ($CH(CH_3)_2$), 20.7 ($C(CH_3)_3$), 29.0 ($C(CH_3)_3$), 49.8 ($CH(CH_3)_2$), 55.2 (OCH_3), 99.9 (aryl-C), 105.8 (aryl-C), 115.0 (aryl-C), 125.7 (aryl-C), 129.3 (*C*N), 140.8 (aryl-C), 156.4 (aryl-C). IR (KBr) $\bar{\nu}$/cm^{-1}: 2961, 2928, 2203, 1593, 1465, 1273, 1273, 1207, 1174, 1105, 1040, 943, 798. UV−vis (toluene) λ_{max}/nm (ε/M^{-1} cm^{-1}): 307 (10 184).

Preparation of [NNN^{sq}]TaCl$_3$ (3). A solution of **1** (0.100 g, 0.17 mmol, 1 equiv) in THF (3 mL) was chilled to −35 °C and added to a cold solution of iodobenzene dichloride (0.023 g, 0.085 mmol, 0.5 equiv) in diethyl ether (5 mL). The reaction mixture was stored overnight at −35 °C. The product precipitated as a blue-green solid and was collected by filtration (0.060 g, 56%). Anal. Calcd for $C_{20}H_{26}Cl_3N_3O_2Ta$: C, 38.27; H, 4.17; N, 6.69. Found: C, 38.59; H, 4.23; N, 6.52. IR (KBr) $\bar{\nu}$/cm^{-1}: 2967, 2928, 1572, 1492, 1459, 1363, 1327, 1262, 1229, 1166, 1105, 1026, 823, 790, 650, 567, 524. UV−vis (benzene) λ_{max}/nm (ε/M^{-1} cm^{-1}): 333 (24 367), 590 (3983).

Preparation of [NNN^{q}]TaCl$_2$(=NPh) (4a). A room-temperature solution of **1** (0.100 g, 0.17 mmol, 1 equiv) in toluene (10 mL) was treated with phenyl azide (0.020 g, 0.17 mmol, 1 equiv). The reaction mixture was stirred for 12 h during which time the product precipitated as violet, microcrystalline solid that was collected by filtration and washed with cyclopentane (0.077 g, 67%). X-ray quality crystals of **4a** were obtained by slowly allowing solutions of **1** and PhN_3 to diffuse together slowly at room temperature. Anal. Calcd for $C_{26}H_{31}Cl_2N_4O_2Ta$: C, 45.69; H, 4.57; N, 8.20. Found: C, 45.49; H, 4.76; N, 8.10 ^{1}H NMR (500 MHz, $CDCl_3$) δ 1.71 (d, 12H, $^3J_{HH} = 6.6$, $CH(CH_3)_2$), 3.95 (s, 6H, OCH_3), 4.82 (sept, 2H, $^3J_{HH} = 6.6$, $CH(CH_3)_2$), 6.52 (d, 2H, $^4J_{HH} = 2.5$, aryl-H), 6.93 (m, 1H, aryl-H), 6.83 (dd, 2H, $^3J_{HH} = 9.8$, $^4J_{HH} = 2.5$, aryl-H), 7.35 (m, 4H, aryl-H), 7.93 (d, 2H, $^3J_{HH} = 9.8$, aryl-H). ^{13}C NMR (125.8 MHz, $CDCl_3$) δ 24.1 ($CH(CH_3)_2$), 55.3 ($CH(CH_3)_2$), 56.0 (OCH_3), 110.0 (aryl-C), 121.3 (aryl-C), 123.6 (aryl-C), 125.3 (aryl-C), 127.9 (aryl-C), 128.1 (aryl-C), 137.5 (aryl-C), 156.1 (aryl-C), 164.8 (aryl-C), 166.2 (aryl-C). IR (KBr) $\bar{\nu}$/cm^{-1}: 2967, 2928, 1593, 1539, 1478, 1448, 1351, 1248, 1201, 1176, 1116, 1015, 817, 768, 695, 582.

Preparation of [NNN^{q}]TaCl$_2$[=N(*p*-C$_6$H$_4$Me)] (4b). Compound **4b** was prepared by a procedure analogous to that used for the preparation of **4a**, starting with 0.100 g of **1** and 0.0023 g of *p*-tolyl azide in 10 mL of toluene. The product was isolated as a dark brown-green microcrystalline solid (0.114 g, 97%). Anal. Calcd for $C_{27}H_{33}Cl_2N_4O_2Ta$: C, 46.50; H, 4.77; N, 8.03. Found: C, 46.75; H, 5.08; N, 7.61. ^{1}H NMR (500 MHz, $CDCl_3$) δ 1.70 (d, 12H, $^3J_{HH} = 6.6$, $CH(CH_3)_2$), 2.45 (s, 3H, aryl-CH_3) 3.94 (s, 6H, OCH_3), 4.81 (m, 2H, $CH(CH_3)_2$), 6.51 (d, 2H, $^4J_{HH} = 2.4$, aryl-H), 6.81 (dd, 2H, $^3J_{HH} = 9.9$, $^4J_{HH} = 2.4$, aryl-H), 7.17 (d, 2H, $^3J_{HH} = 8.2$, aryl-H), 7.23 (d, 2H, $^3J_{HH} = 8.2$, aryl-H), 7.92 (d, 2H, $^3J_{HH} = 9.9$, aryl-H). ^{13}C NMR (125.8 MHz, $CDCl_3$) δ 24.1 ($CH(CH_3)_2$), 47.1 (aryl-CH_3), 55.3 ($CH(CH_3)_2$), 55.9 (OCH_3), 95.0 (aryl-C), 115.3 (aryl-C), 121.1 (aryl-C), 125.2 (aryl-C), 127.6 (aryl-C), 128.6 (aryl-C), 133.2 (aryl-C), 137.4 (aryl-C), 166.1 (aryl-C), 176.1 (Ar−C). IR (KBr) $\bar{\nu}$/cm^{-1}: 2968, 2929, 1591, 1448, 1367, 1350, 1322, 1259, 1231, 1212, 1122, 1015, 810, 691, 585, 511.

Preparation of [NNN^{q}]TaCl$_2$[=N(*p*-C$_6$H$_4$^{t}Bu)] (4c). Compound **4c** was prepared by a procedure analogous to that used for the preparation of **4a**, starting with 0.100 g of **1** and 0.0038 g of *p-tert*-butylphenyl azide in 10 mL of toluene. The product was isolated as a dark brown-green microcrystalline solid (0.087 g, 70%). Anal. Calcd for $C_{30}H_{39}Cl_2N_4O_2Ta$: C, 48.72; H, 5.32; N, 7.58. Found: C, 47.44; H, 5.35; N, 7.28. ^{1}H NMR (500 MHz, $CDCl_3$) δ 1.33 (s, 9H, $C(CH_3)_3$), 1.72 (d, 12H, $^3J_{HH} = 6.6$, $CH(CH_3)_2$), 3.94 (s, 6H, OCH_3), 4.82 (m, 2H, $CH(CH_3)_2$), 6.51 (d, 2H, $^4J_{HH} = 2.2$, aryl-H), 6.80 (dd, 2H, $^3J_{HH} = 9.8$, $^4J_{HH} = 2.2$, aryl-H), 7.23 (d, 2H, $^3J_{HH} =$ 8.4, aryl-H), 7.40 (d, 2H, $^3J_{HH} = 8.4$, aryl-H), 7.90 (d, 2H, $^3J_{HH} =$ 9,8, aryl-H). ^{13}C NMR (125.8 MHz, $CDCl_3$) δ 24.0 ($CH(CH_3)_2$), 31.6 ($C(CH_3)_3$), 34.2 ($C(CH_3)_3$), 55.3 ($CH(CH_3)_2$), 55.9 (OCH_3), 95.1 (aryl-C), 121.0 (aryl-C), 124.6 (aryl-C), 125.2 (aryl-C), 127.2 (aryl-C), 137.4 (aryl-C), 146.3 (aryl-C), 153.6 (aryl-C), 164.7 (aryl-

Table 1. X-ray Diffraction Data-Collection and Refinement Parameters for **1**, **4a**, and **5**

	[NNN^{cat}]TaCl$_2$ (**1**)	[NNN^{q}]Ta(=NPh)Cl$_2$ (**4a**)	[NNN^{q}]Ta(=NNCPh$_2$)Cl$_2$ (**5**)
empirical formula	$C_{20}H_{26}Cl_2N_3O_2Ta$	$C_{26}H_{31}N_4O_2Cl_2Ta$	$C_{36.5}H_{44}Cl_2N_5O_2Ta$
fw	592.29	683.40	826.80
cryst syst	tetragonal	triclinic	triclinic
space group	$I4_1/a$	$P\bar{1}$	$P\bar{1}$
a/Å	15.8698(14)	9.3551(6)	14.5899(6)
b/Å	15.8698(14)	9.8430(7)	15.5056(6)
c/Å	16.8680(14)	14.4426(10)	16.2442(7)
α/deg	90	94.5768(8)	80.1400(5)
β/deg	90	97.6611(8)	73.7726(5)
γ/deg	90	92.9604(9)	87.8341(5)
V/Å^3	4248.2(6)	1311.22(15)	3476.3(2)
Z	8	2	4
reflns collected	23 533	15 765	44 070
independent reflns (R_{int})	2320 (0.0489)	6429 (0.0175)	17 693 (0.0183)
R1 ($I > 2\sigma(I)$)	0.0187	0.0249	0.0189
wR2 (all data)	0.0513	0.0631	0.0470

Scheme 1. Synthesis of [NNN^{cat}]H$_3$

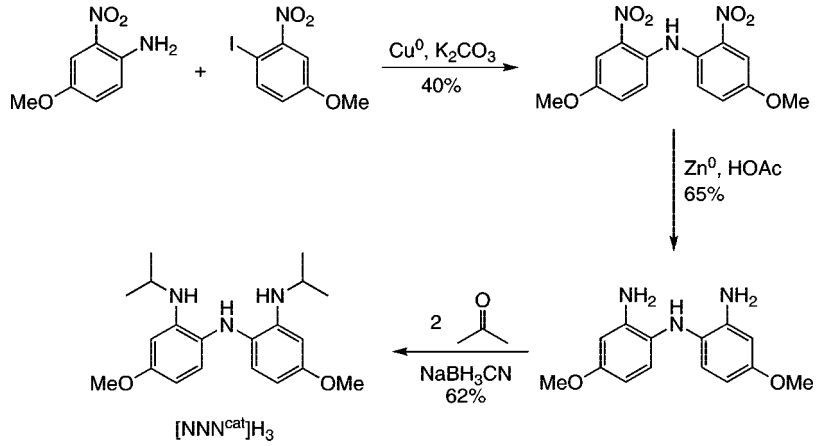

C), 166.0 (aryl-C). IR (KBr) $\bar{\nu}$/cm^{-1}: 2961, 1596, 1492, 1451, 1355, 1253, 1201 1119, 1015, 798. UV−vis (THF) λ_{max}/nm (ε/M^{-1} cm^{-1}): 314 (20 492), 375 (11 781), 462 (9714), 786 (10 900).

Preparation of [NNN^{q}]TaCl$_2$(=NNCPh$_2$) (5). A solution of **1** (0.200 g, 0.34 mmol, 1 equiv) in toluene (10 mL) was chilled to −35 °C and added to a cold solution of diphenyldiazomethane (0.069 g, 0.38 mmol, 1.2 equiv) in toluene (5 mL). After solution was stirred overnight, the volatiles were removed under reduced pressure. The solid residue was washed with pentane (3 × 10 mL) to give a dark brown-green solid (0.169 g, 60%). X-ray quality crystals were obtained from reaction. ^{1}H NMR (500 MHz, $CDCl_3$) δ 1.42 (d, 12H, $^3J_{HH}$ = 5.2, CH(CH_3)$_2$), 3.89 (s, 6H, OCH$_3$), 4.59 (m, 2H, CH(CH$_3$)$_2$) 6.39 (s, 2H, aryl-H), 6.76 (d, 2H, $^3J_{HH}$ = 9.5, aryl-H), 7.36 (m, 8H, aryl-H), 7.80 (m, 2H, aryl-H), 7.85 (d, 2H, $^3J_{HH}$ = 9.5). ^{13}C NMR (125.8 MHz, $CDCl_3$) δ 23.1 (CH(CH_3)$_2$), 54.9 (CH(CH$_3$)$_2$), 55.9 (OCH$_3$), 95.2 (NCPh_2), 109.9 (aryl-C), 113.1 (aryl-C), 120.7 (aryl-C), 125.1 (aryl-C), 127.8 (aryl-C), 128.3 (aryl-C), 129.1 (aryl-C), 131.1 (aryl-C), 137.3 (aryl-C), 164.3 (aryl-C), 165.8 (aryl-C). IR (KBr) $\bar{\nu}$/cm^{-1}: 2961, 1593, 1443, 1253, 1204, 116, 1015, 801, 694, 578. UV−vis (toluene) λ_{max}/nm (ε/M^{-1} cm^{-1}): 300 (27 615).

Crystallographic Procedures. X-ray diffraction data were collected on crystals mounted on glass fibers using a Bruker CCD platform diffractometer equipped with a CCD detector. Measurements were carried out at 163 K using Mo Kα (λ = 0.71073 Å) radiation, which was wavelength-selected with a single-crystal graphite monochromator. The SMART program package was used to determine unit-cell parameters and to collect data.[20] The raw frame data were processed using SAINT[21] and SADABS[22] to yield the reflection data files. Subsequent calculations were carried out using the SHELXTL program suite.[23] Structures were solved by direct methods and refined on F^2 by full-matrix least-squares techniques. Analytical scattering factors for neutral atoms were used throughout the analyses.[24] Hydrogen atoms were included using a riding model. ORTEP diagrams were generated using ORTEP-3 for Windows.[25] Diffraction data are shown in Table 1.

Results

Synthesis and Metalation of [NNN^{cat}]H$_3$. The redox-active tris(amide) ligand bis(2-isopropylamino-4-methoxyphenyl)amine ([NNN^{cat}]H$_3$) was prepared in modest yields by a three-step procedure starting from 4-methoxy-2-nitroaniline and 1-iodo-4-methoxy-2-nitrobenzene (Scheme 1). A modified Ullmann coupling was used to construct the ligand backbone. The presence of electron-donating methoxy groups on both coupling components required the use of excess copper powder to achieve satisfactory yields of the coupled products. Coupling reactions between substrates without electron-donating methoxy substit-

(20) *SMART Software Users Guide, Version 5.1*; Bruker Analytical X-ray Systems, Inc.: Madison, WI, 1999.
(21) *SAINT Software Users Guide, Version 6.0*; Bruker Analytical X-ray Systems, Inc.: Madison, WI, 1999.
(22) Sheldrick, G. M. *SADABS, Version 2.10*; Bruker Analytical X-ray Systems, Inc.: Madison, WI, 2002.
(23) Sheldrick, G. M. *SHELXTL, Version 6.12*; Bruker Analytical X-ray Systems, Inc.: Madison, WI, 2001.
(24) *International Tables for X-ray Crystallography*; Kluwer Academic Publishers: Dordrecht, The Netherlands, 1992; Vol. C.
(25) Farrugia, L. J. *J. Appl. Crystallogr.* **1997**, *30*, 565.

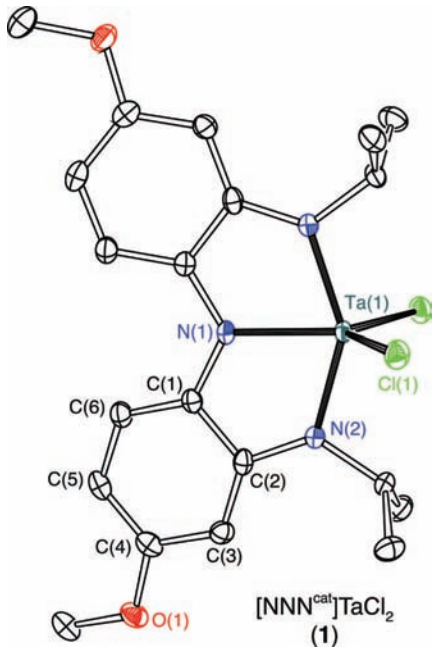

Figure 1. ORTEP diagram of $[NNN^{cat}]TaCl_2$ (**1**). Thermal ellipsoids are drawn at 50%, and hydrogen atoms are omitted for clarity.

uents have been achieved in high yields without the use of copper;[26] however, in this case, copper was needed for the formation of the product. Reduction of bis(4-methoxy-2-nitrophenyl)amine was readily achieved using zinc and glacial acetic acid, and a subsequent reductive amination using the mild reductant sodium cyanoborohydride afforded the target ligand. The pure ligand is sensitive to oxidation, and even short exposure to air results in a color change from pale yellow to violet; however, the ligand is stable for months when stored at −35 °C in a glovebox.

Coordination of $[NNN^{cat}]H_3$ was readily achieved using the trimethyl tantalum synthon, $TaCl_2Me_3$, developed by Schrock and co-workers.[18] The reaction of $[NNN^{cat}]H_3$ with $TaCl_2Me_3$ in cold ether was indicated by a color change from pale yellow to deep red with the only byproduct of the reaction being methane. Removal of the solvent and washing of the brick red residue with cold cyclopentane afforded pure product, identified as **1**, in virtually quantitative yield. Characterization of **1** by ^{1}H NMR spectroscopy suggested a C_{2v}-symmetric complex as evidenced by a doublet resonance at 1.35 ppm and a septet resonance at 4.54 ppm, corresponding to the methyl and methine protons of the ligand isopropyl groups. Similarly, only one methoxy resonance and three aryl resonances were observed for the ligand.

Single-crystal X-ray diffraction studies confirmed a five-coordinate trigonal bipyramidal geometry for **1**. Dark-red, needle crystals of **1** were obtained from chilled cyclopentane solutions of the complex. Complex **1** crystallized in the tetragonal space group $I4_1/a$, with half of the molecule defining the asymmetric unit. As shown in Figure 1, the $[NNN^{cat}]^{3-}$ ligand coordinates in a meridional fashion to the tantalum center. The isopropylamide groups occupy axial positions of a trigonal bipyramid with the equatorial plane occupied by the diphenyl amide of $[NNN^{cat}]^{3-}$ and the two chloride ligands. Selected metrical parameters for **1** are collected in Table 2. All tantalum−ligand bond lengths are in the normal range for a tantalum(V) complex. Carbon−nitrogen and carbon−carbon distances within the $[NNN^{cat}]^{3-}$ ligand are consistent with C−N single bonds and aromatic phenyl ring. A O(1)−C(4) distance of 1.37 Å is consistent with a single bond. The fused five-membered ring system resulting from coordination of $[NNN^{cat}]^{3-}$ to the metal center results in an acute N(1)−Ta(1)−N(2) angle; however, the three equatorial substituents adopt ideal angles of 120°.

Table 2. Selected Bond Distances (Å) and Angles (deg) for $[NNN^{cat}]TaCl_2$ (**1**)

Bond Distances/Å	
Ta(1)−N(1)	2.082(3)
Ta(1)−N(2)	1.963(2)
Ta(1)−Cl(1)	2.3348(7)
N(1)−C(1)	1.423(3)
N(2)−C(2)	1.383(3)
C(1)−C(2)	1.414(4)
C(2)−C(3)	1.385(4)
C(3)−C(4)	1.391(4)
C(4)−C(5)	1.390(4)
C(5)−C(6)	1.401(4)
C(6)−C(1)	1.383(4)
O(1)−C(4)	1.376(3)
Bond Angles/deg	
N(1)−Ta(1)−N(2)	73.52(6)
N(1)−Ta(1)−Cl(1)	119.642(17)
N(2)−Ta(1)−Cl(1)	97.42(7)
Cl(1)−Ta(1)−Cl(1)′	120.72(3)

Five-coordinate **1** reacted with the strong σ-donor ligand ^{t}BuNC to afford the six-coordinate adduct **2**, as shown in Scheme 2. Addition of neat ^{t}BuNC to a toluene solution of **1** results in a slight color change from brick red to burgundy. The product, **2**, was isolated as a red-purple solid after removal of the solvent and washing of the residue with cyclopentane to remove residual isonitrile. The ^{1}H NMR spectra of **1** and **2** are very similar, with only small changes in chemical shift values for most resonances. The most diagnostic change in the ^{1}H NMR spectra occurred for the isopropyl methine resonances. Upon coordination of the isonitrile ligand the methine septet shifts from 4.54 ppm as observed in **1** to 5.57 ppm as observed in **2**. It is worth noting that while coupling was readily observed within the isopropyl groups of **1**, in **2** the coupling is not well resolved, suggesting that the nitrile ligand may be dissociating reversibly in solution. The spectrum of **2** showed a singlet at 0.59 ppm, which integrated to a single, coordinated *tert*-butyl isonitrile ligand. The solid-state IR spectrum of **2** confirmed the coordination of the isonitrile to the tantalum complex. The C≡N stretch was observed at 2203 cm^{-1}, which is shifted to higher frequency of the free isonitrile (2125 cm^{-1}). In contrast to the reaction of **1** with isonitrile, we found no evidence of CO binding to the tantalum center, even for solutions of the complex under a CO atmosphere.

One-Electron Oxidation of 1. On the basis of our success using halogen oxidations to probe the redox reactivity of d^0 metal complexes with redox-active ligands,[9] we investigated the halogen oxidation of **1**. Addition of 0.5 equiv of the chlorine surrogate $PhICl_2$ to a cold ethereal solution of **1** resulted in an immediate color change from red to dark green. The reaction mixture was stored at −35 °C overnight, resulting in the precipitation of **3** as a microcrystalline green-blue solid. A strong absorbance, observed at 590 nm (3983 M^{-1} cm^{-1}), in the UV−vis spectrum of **3** is consistent with a one-electron-oxidized ligand;[27] a paramagnetic species was further suggested by NMR spectroscopy, which revealed a spectrum that was paramag-

(26) Jones, M. B.; MacBeth, C. M. *Inorg. Chem.* **2007**, *46*, 8117–8119.

Scheme 2. Synthesis and Reactivity of [NNN^{cat}]TaCl$_2$ (**1**)

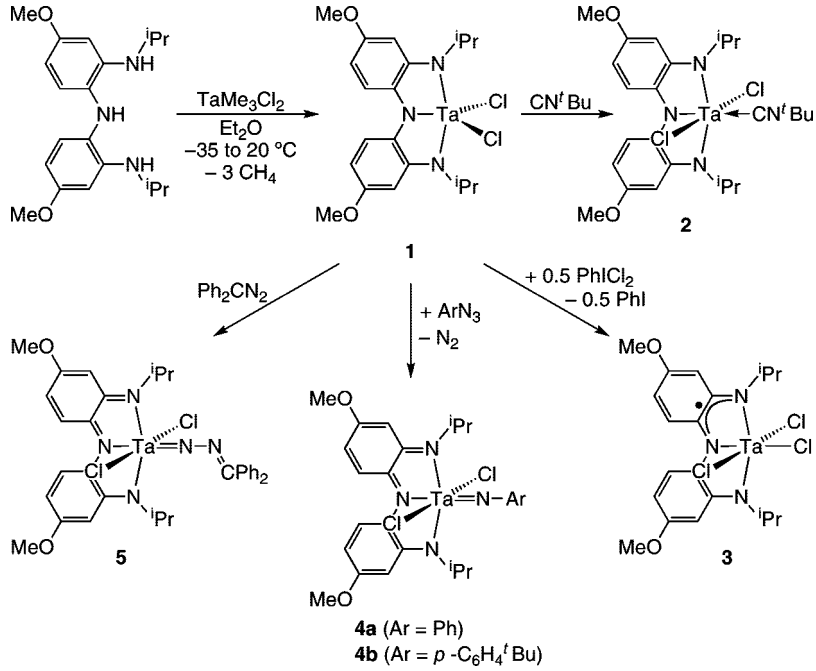

netically broadened into the baseline. The room-temperature EPR spectrum of **3** in toluene, provided in Figure 2, showed an eight-line pattern centered at $g = 1.897$, consistent with a single unpaired electron coupling to the $I = 7/2$ tantalum center. These data are analogous to the related [ONO$^{sq\bullet}$]TaCl$_3$ complex,[11] which we have characterized crystallographically, suggesting that **3** is six-coordinate octahedral species depicted in Scheme 2, with a radical [NNN$^{sq\bullet}$]$^{2-}$ ligand and three chloride ligands in a meridional arrangement.

Cyclic voltammetry experiments were used to probe the redox properties of the tantalum redox-active-ligand platform. The response features of the cyclic voltammogram of **3**, shown in Figure 3, revealed two reversible one-electron processes and an irreversible oxidation at higher potential. A reversible, one electron oxidation was observed at 0.15 V (vs [Cp$_2$Fe]$^{+/0}$). The ΔE_p for this redox couple is 94 mV, and the value is independent of scan rate over 50−1600 mV/s. The anodic to cathodic peak current ratio (i_{pa}/i_{pc}) is unity over all scan rates and a plot of i_{pc} vs (sweep rate)$^{1/2}$ is linear, indicative of a diffusion-controlled, reversible, one-electron transfer process. Similarly, a reversible, diffusion-controlled, one-electron, reduction was observed at −0.32 V ($i_{pc}/i_{pa} = 1.1$; $\Delta E_p = 90$ mV at 200 mV/s). Our interpretation of these results is summarized in eq 1: one-electron reduction of **3** generates the {[NNN^{cat}]TaCl$_3$}$^-$ monoanion, whereas one-electron oxidation generates the {[NNN^{q}]TaCl$_3$}$^+$ monocation. A second oxidation was observed at $E_{pa2} = 1.5$ V, and is irreversible with an $|E_p - E_{p/2}|$ value of 96 mV at 200 mV/s. This is indicative of a reversible electron transfer followed by a fast chemical reaction. Though a linear plot of i_{pc} vs (sweep rate)$^{1/2}$ indicated the electron transfer is diffusion-controlled, this oxidation peak is close to the solvent limit; hence, we are uncertain if the apparent increased peak height is due to a two-electron oxidation process or interference from the electrolyzed solvent system. It is noteworthy that the one-electron processes relating the three stable ligand oxidation states are relatively close in energy, $\Delta E^{\circ\prime} = 0.5$ V. For comparison, electrochemical studies of copper and zinc complexes of the related [ONO$^{sq\bullet}$]$^{2-}$ ligand showed that the one-electron oxidation and reduction process are separated by greater than 0.9 V.[28]

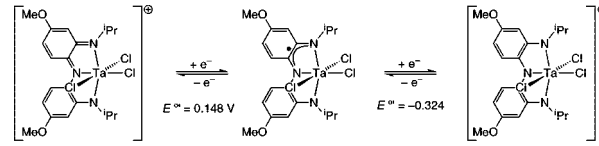

(1)

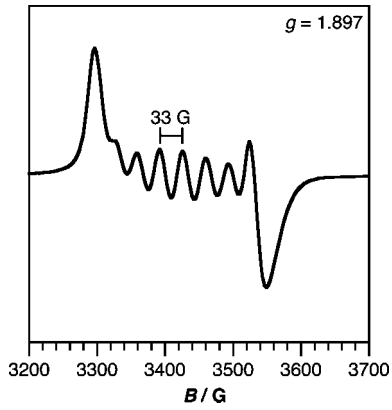

Figure 2. Room-temperature EPR spectrum of [NNN$^{sq\bullet}$]TaCl$_3$ (**3**) in toluene.

Two-Electron Nitrene Transfer to 1. The reversible one-electron oxidation of **3** observed in the electrochemical experiments suggested that net two-electron oxidation reactivity might be possible from **1**. Accordingly, when a solution of **1** was treated with phenyl azide, the color changed from red to purple with concomitant gas evolution and precipitation of a violet microcrystalline solid, identified as **4a**, (Scheme 2). The ^{1}H

(27) Carter, S. M.; Sia, A.; Shaw, M. J.; Heyduk, A. F. *J. Am. Chem. Soc.* **2008**, *130*, 5838–5839.

(28) (a) Chaudhuri, P.; Hess, M.; Hildenbrand, K.; Bill, E.; Weyhermüller, T.; Wieghardt, K. *Inorg. Chem.* **1999**, *38*, 2781–2790. (b) Chaudhuri, P.; Hess, M.; Weyhermüller, T.; Wieghardt, K. *Angew. Chem., Int. Ed.* **1999**, *38*, 1095–1098.

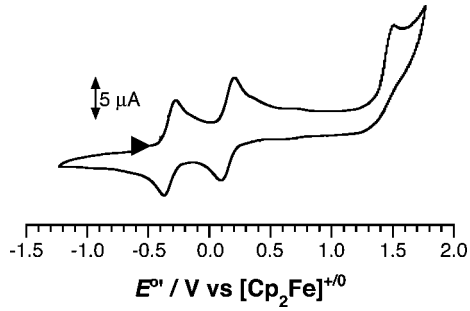

Figure 3. Cyclic voltammogram of 1 mM [NNN$^{sq\bullet}$]$TaCl_3$ (**3**) in CH_2Cl_2 (0.1 M [$^nBu_4N$][PF_6]). Conditions: platinum disk working electrode, scan rate 200 mV/s.

NMR spectrum of **4a**, which is consistent with a C_{2v}-symmetric molecule, is indicative of ligand oxidation and transfer of the phenyl nitrene to the tantalum center. Both the methyl and methine resonances for the isopropyl groups shift by ~0.3 ppm to higher frequency. The changes in the ^{1}H NMR resonances for the ligand backbone are even more dramatic. The viscinal protons shift downfield by greater than 0.6 ppm, resonating at 6.83 and 6.93 ppm, while the third aromatic proton shifts upfield by 0.1 ppm, resonating at 6.52 ppm. The methoxy proton resonance also shifts 0.5 ppm downfield to 3.95 ppm. Analogous results were obtained using *p*-$MeC_6H_4N_3$ and *p*-$^tBuC_6H_4N_3$ to afford **4b** and **4c**, respectively. The ^{1}H NMR spectra of **4b** and **4c** are identical to that of **4a** except for the resonances associated with the *p*-tolyl and *tert*-butylphenyl groups of the imido ligands.

The solid-state molecular structure of **4a** was determined by X-ray diffraction experiments. X-ray quality, violet crystals of **4a** were obtained by diffusing solutions of **1** and PhN_3 together slowly at room temperature. Complex **4a** crystallizes in the triclinic space group $P\bar{1}$ with a single molecule in the asymmetric unit. As shown in Figure 4, the tantalum center in **4a** is distorted octahedral with two trans chloride ligands and the phenyl imido ligand in a meridional arrangement. Selected metrics for the tantalum coordination sphere are given in Table 3. The redox-active ligand is planar, and the intraligand and metal−ligand bond lengths indicate oxidation of the ligand by two electrons to the [NNN^q]$^-$ form. The ligand C−N bond distances in **4a** are contracted by an average of 0.045 Å relative to the C−N distances in **1**, while the C(1)−C(2) and C(11)−C(12) distances in **4a** are stretched by nearly the same amount. Alternating C−C bond lengths within the six-membered rings of the [NNN^q]$^-$ ligand are indicative of cyclohexadiene character and the two-electron oxidation state of the ligand. Notably, the C−O bonds of the 4-methoxy groups also are contracted by 0.02 Å in **4a**. Bond distances between the [NNN^q]$^-$ ligand and the tantalum center increase by nearly 0.2 Å in **4a**, consistent with a decrease in Coulombic attraction between the metal and ligand that occurs upon oxidation of the ligand. Finally, the Ta−N(imido) bond distance is relatively long at 1.80 Å and the Ta−N−C angle is nearly linear at 167°.

Attempts to transfer diphenylcarbene from diphenyldiazomethane to **1** instead resulted in the formation of a diphenylmethylidenehydrazido complex as shown in Scheme 2. Addition of 1 equiv of N_2CPh_2 to a solution of **1** resulted in a color change consistent with oxidation of the tantalum complex; however, no gas evolution was observed. The ^{1}H NMR spectrum of the product suggested a species analogous to imido complexes **4a** and **4b** with the incorporation of a single diphenylmethylene fragment. Notably, the ^{13}C NMR spectrum did not show a

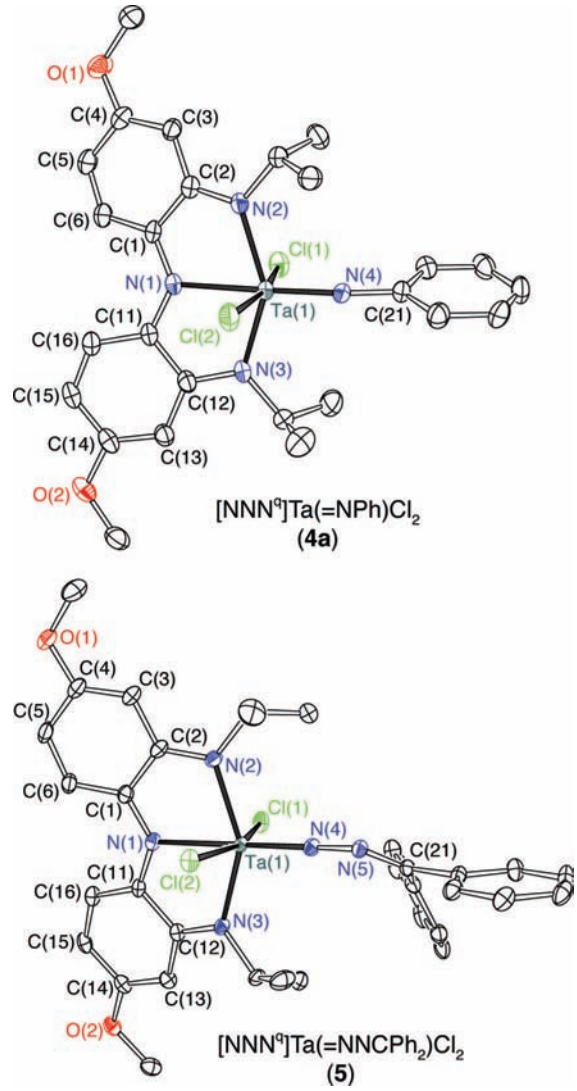

Figure 4. ORTEP diagrams of [NNN^q]Ta(=NPh)Cl_2 (**4a**) and [NNN^q]-Ta(=NNCPh_2)Cl_2·1/2C_6H_5Me (**5**·1/2C_6H_5Me). Ellipsoids are drawn at 50% probability. Hydrogen atoms and the solvent molecule of **5**·1/2C_6H_5Me are omitted for clarity.

resonance in the alkylidene region ($\delta \geq 200$ ppm),[29] providing a second clue that carbene transfer to the tantalum center did not occur.

The product was characterized as **5** on the basis of the results of X-ray diffraction studies. Figure 4 shows the molecular structure of **5** as determined by X-ray diffraction. As shown in Table 3, the metrical parameters for the tantalum coordination sphere in **5** are largely consistent with those observed in **4a**. Similarly, the intraligand C−N, C−C, and C−O bond distances are all consistent with oxidation of the redox-active ligand to the [NNN^q]$^-$ state. The Ta−N bond distance in **5** is 1.8 Å and the Ta−N−N bond angle is 167°, consistent with the metrical data for **4a**. The α-nitrogen, N(4) must have significant *sp* character, which would be expected to reduce the N−N bond order. Consistent with this hypothesis is the N−N distance of 1.34 Å, which is in between the double bond N=N distance observed in PhN=NPh (1.26 Å)[30] and the single-bond N−N distance observed Ph_2C=N−N=CPh_2 (1.40 Å).[31] The *β*-nitro-

(29) Schrock, R. R. *Acc. Chem. Res.* **1979**, *12*, 98–104.
(30) Brown, C. J. *Acta Crystallogr.* **1966**, *21*, 146–152.

Table 3. Selected Bond Distances (Å) and Angles (deg) for **4a** and **5**

	Bond Distances/Å	
	$[NNN^q]Ta(=NPh)Cl_2$ (**4a**)	$[NNN^q]Ta(=NNCPh_2)Cl_2$ (**5**)[a]
Ta(1)−N(1)	2.277(3)	2.2712(15)
Ta(1)−N(2)	2.135(3)	2.1488(16)
Ta(1)−N(3)	2.116(3)	2.0964(15)
Ta(1)−N(4)	1.802(3)	1.8038(15)
Ta(1)−Cl(1)	2.4420(8)	2.4466(5)
Ta(1)−Cl(2)	2.4214(8)	2.4302(5)
N(4)−N(5)	−	1.344(2)
N(5)−C(21)	−	1.302(2)
Bond Angles/deg		
N(1)−Ta(1)−N(2)	73.07(9)	73.84(6)
N(1)−Ta(1)−N(3)	73.80(10)	74.80(6)
N(1)−Ta(1)−N(4)	73.52(11)	177.21(6)
N(1)−Ta(1)−Cl(1)	81.17(7)	81.73(4)
N(1)−Ta(1)−Cl(2)	86.77(7)	81.86(4)
Ta(1)−N(4)−C(21)	167.9(2)	−
Ta(1)−N(4)−N(5)	−	167.27(13)
N(4)−N(5)−C(21)	−	120.55(15)

[a] Average values for the two inequivalent molecules of **5** in the asymmetric unit.

gen, N(5), remains sp^2-hybridized as indicated by an N−N−C angle of less than 121° and a short N═C bond of 1.31 Å.

Discussion

Ligand Design and Synthesis. The synthetic strategy used for the $[NNN^{cat}]H_3$ ligand platform is straightforward and allows for ready modification of both the electronic and steric properties of the ligand. In this work, a highly reducing ligand with moderate steric protection for the metal was targeted. Incorporation of isopropyl substituents on the 2 and 2′ amine groups provided enough steric protection at the metal center to avoid dimer formation, as we have observed with related tantalum chemistry.[11] Initially, we had attempted to incorporate *tert*-butyl groups via Cummins' elegant method using d_6-acetone and methyllithium;[32] however, these efforts were frustrated by cyclization of the isopropylimine to form a benzimidazolidene species.[33] This cyclization circumvented isolation of the diimine derivative and necessitated the in situ reductive condensation with sodium cyanoborohydride presented in Scheme 1.

To maximize the reducing power of the $[NNN^{cat}]^{3-}$ ligand, methoxy groups were incorporated into the 4 and 4′ positions of the diphenylamine backbone. In addition to providing steric protection to the ligand backbone, in the oxidized form of the ligand, $[NNN^q]^-$, the methoxy groups are in resonance with the 2-isopropylimine nitrogen atoms as shown in eq 2. The solid state structures of **4a** and **5** suggest the importance of resonance structure B, in that a significant contraction in the C−O bond is observed in the structures of both oxidized complexes **4a** and **5**. Similarly, the ^{1}H NMR resonances for the methoxy groups in **4a**−**c** and **5** all shift downfield, suggesting a decrease in electron density at the oxygen upon oxidation. It is worth noting that the solid-state structures, as well as the NMR spectroscopic data, suggest that the oxidized $[NNN^q]^-$ ligand in **4a**−**c** and **5** is symmetric, as would be expected for equal contributions from the equivalent A/A′ and B/B′ resonance structures of eq 2. This is somewhat different that the related $[ONO^q]^-$ ligand, which has been observed to have a localized cyclohexadienediimine when coordinated to tantalum[11] and other metals.[34]

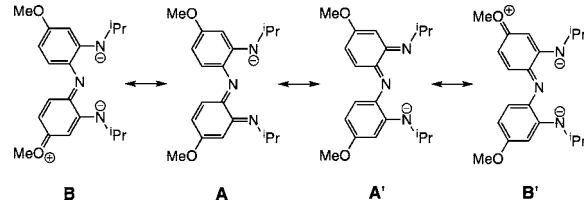

(2)

Mixing of Metal and Ligand Valence Electrons. The spectroscopic data presented here suggest significant delocalization of the ligand valence electrons onto the tantalum center for complexes **1**, **2**, and **3**. Similar valence-electron delocalization has been studied extensively for ruthenium complexes with redox-active ligands.[35] The metrical parameters observed for complex **1** are consistent with a formal tantalum(V) oxidation state with the fully reduced $[NNN^{cat}]^{3-}$ ligand. However, the brick red color of **1** deriving from a strong electronic absorbance at 311 nm, which tails into the visible region, suggests significant ligand-to-metal charge transfer in the complex. In an attempt to highlight any tantalum(III) character in **1**, we sought to prepare its CO adduct; however, we found no evidence for interaction of the weak σ-donor, strong π-acid ligand with the tantalum center. On the other hand, *tert*-butylisonitrile readily coordinated to the tantalum center of **1** to form **2**. Binding of the isonitrile to tantalum resulted in an increase in the isonitrile stretching frequency from 2125 to 2203 cm^{-1}, an effect that is well established in the literature.[36] The C≡N stretching frequency in **2** is lower than that observed for the 16-electron tantalum complex, $Cp^*Ta^VCl_4(CN^tBu)$ (2241 cm^{-1}),[37] but is higher than that observed for the 18-electron tantalum complex, $Cp^*_2Ta^{III}(\eta^1$-butadiene)(CN^tBu) (2164 cm^{-1}).[38] In fact, the C≡N stretching frequency for **2** is comparable to that observed for $Cp^*Ta^VCl_2(=N^tBu)(CN^tBu)$ (2200 cm^{-1}),[39] which can be considered either a 16-electron or an 18-electron complex depending on whether the imido ligand is counted as a 4-electron or as a 6-electron donor. These comparisons suggest that **2** is best described as a tantalum(V) complex in which the $[NNN^{cat}]^{3-}$ ligand acts as a very strong π-donor toward the metal center.[40]

The room-temperature solution EPR spectrum of **3** provided further evidence for delocalization of the ligand valence orbitals onto the tantalum center. A purely tantalum-localized radical

(31) Wolstenholme, D. J.; Cameron, T. S. *J. Phys. Chem. A* **2006**, *110*, 9870–9878.
(32) Johnson, A. R.; Cummins, C. C.; Gambarotta, S. *Inorg. Synth.* **1998**, *32*, 123–132.
(33) Gorelik, M. V.; Han, I.-H.; Lomzakova, V. I.; Korolev, B. A. *Z. Org. Khim.* **1976**, *12*, 177–186.
(34) McGarvey, B. R.; Ozarowski, A.; Tian, Z.; Tuck, D. G *Can. J. Chem.* **1995**, *73*, 1213–1222.
(35) (a) Pierpont, C. G *Coord. Chem. Rev.* **2001**, *216*−*217*, 99–125. (b) Gorelsky, S. I.; Dodsworth, E. S.; Lever, A. B. P.; Vlcek, A. A. *Coord. Chem. Rev.* **1998**, *174*, 469–494. (c) Masui, H.; Lever, A. B. P.; Auburn, P. R. *Inorg. Chem.* **1991**, *30*, 2402–2410.
(36) Coordination of isonitriles to d^0 metals normally increases the stretching frequency. For a discussion of this effect see Guo, Z. Y.; Swenson, D. C.; Guram, A. S.; Jordan, R. F *Organometallics* **1994**, *13*, 766–773.
(37) Gomez, M.; Gomez-Sal, P.; Nicolas, M. P.; Royo, P. *J. Organomet. Chem.* **1995**, *491*, 121–125.
(38) Strauch, H. C.; Wibbeling, B.; Frohlich, R.; Erker, G.; Jacobsen, H.; Berke, H. *Organometallics* **1999**, *18*, 3802–3812.
(39) Royo, P.; Sanchez-Nieves, J. *J. Organomet. Chem.* **2000**, *597*, 61–68.
(40) It is tempting to assign the $[NNN^{cat}]^{3-}$ ligand as a 12-electron donor ($6\sigma + 6\pi$ electrons), to make complex **2** an 18-electron tantalum(V) complex; however, the three π-symmetry lone pairs of the $[NNN^{cat}]^{3-}$ ligand interact with only two metal d orbitals, limiting the ligand to be a 10-electron donor ($6\sigma + 4\pi$).

(i.e., Ta^{IV}) would show an isotropic signal with a diagnostic eight-line pattern owing to hyperfine coupling with the $I = 7/2$ tantalum nucleus,[41] whereas a purely ligand-centered radical (i.e., $[NNN^{sq\bullet}]^{2-}$) would show an isotropic signal with hyperfine coupling to the H and N nuclei of the ligand.[27] In the case of **3**, the room-temperature EPR signal is observed at $g = 1.897$. The signal appears as an eight-line pattern consistent with coupling to the tantalum nucleus ($A_{iso} = 31$ G). The signal also shows significant intensity localized in the outermost peaks of the signal, consistent with the single derivative signal expected for a ligand-based radical. These data are consistent with delocalization of the unpaired electron in **3** over the entire molecule. Equation 3 shows the two extreme resonance structures representative of this delocalization. For comparison, recent EPR studies of tantalum(IV) sandwich compounds show an eight-line isotropic pattern with much larger isotropic hyperfine coupling constants ($A_{iso} = 61-113$ G).[42] The variation in these values was attributed to electron delocalization, with higher A_{iso} values corresponding to more localization of the electron on the metal. Similarly, in the case of **3**, while the eight-line pattern shown in Figure 2 provides unequivocal evidence for delocalization of the radical onto the tantalum center, the relatively small magnitude of the hyperfine coupling constant suggests the dominant resonance structure is $[NNN^{sq\bullet}]Ta^{V}Cl_3$.

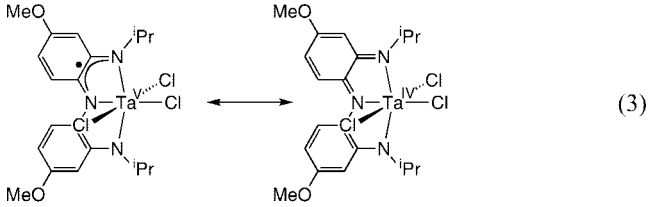

$[NNN^{sq\bullet}]Ta^{V}Cl_3$ $[NNN^{q}]Ta^{IV}Cl_3$ (3)

Oxidation and Nitrene-Transfer Reactions of 1. In previous studies, we have found halogen oxidation reactions to be useful probes of the redox reactivity of d^0 metal complexes with redox-active ligands. In the case of **1**, the addition of 0.5 equiv of the chlorine surrogate $PhICl_2$ gave a rapid reaction and the formation of the open-shell radical **3**. We were surprised to find that the addition of 1 equiv of $PhICl_2$ (i.e., 1 equiv of Cl_2 per equiv of **1**) to **1** did not result in the formation of the expected $[NNN^{q}]TaCl_4$ species as we had observed previously in related tantalum chemistry.[11] Two factors may play a role in thwarting further chlorine oxidation of **3**. First, an oxidation potential of +0.15 V measured for **3** suggests that chlorine may not be a powerful enough oxidant to generate the putative $[NNN^{q}]TaCl_4$ species (Cl_2 $E^{\circ\prime} = 0.18$ V vs $[Cp_2Fe]^{+/0}$).[19] The second factor may be steric. In the case of $[ONO^{q}]TaCl_4$,[11] the complex adopts a pentagonal bipyramidal geometry, with the tridentate $[ONO^{q}]^{-}$ ligand and two halides in the equatorial plane. A similar geometry with the $[NNN^{q}]^{-}$ ligand would be inhibited by the increased steric bulk of the isopropylimine groups, which would need to be accommodated in the equatorial plane of a putative $[NNN^{q}]TaCl_4$ structure.

Despite the difficulty in performing a two-electron chlorine oxidation of **1**, the two-electron oxidation of **1** to form tantalum imido complexes occurs readily. Addition of aryl azides to **1** results in the release of N_2 and formation of the tantalum-imido linkage with concomitant two-electron oxidation of the redox-active ligand. Studies of nitrene transfer from an organic azide to a tantalum(III) complex have shown that nitrene transfer proceeds through initial coordination of the α-nitrogen of the organic azide.[43] Our results with diphenyldiazomethane suggest a similar pathway. In the case of azide addition to **1** to form **4a**−**c**, initial binding of the α-nitrogen may lead to coordination of the γ-nitrogen and N_2 extrusion. Conversely, after formation of **5** from Ph_2CN_2 and **1**, methylidene transfer may not occur because of unfavorable steric interactions between the isopropyl groups of the $[NNN^{q}]^{-}$ ligand and the phenyl groups of the methylidene fragment.

The metrical parameters for tantalum imido complexes **4a** and **5** are consistent with limited Ta−imido triple bond character. The Ta−N distances in **4a** and **5** are longer than expected both from estimates of the Ta^{V} and N radii ($d_{Ta-N} = 1.75$ Å),[1] and from comparison to tantalum−imido complexes in the literature;[44] however, the Ta−N−C and Ta−N−N bond angles in **4a** and **5** are fairly linear. Despite the elongation of the tantalum imido linkage in **4a** (and presumably **4b** and **4c**), the functional group appears to be relatively robust. Solutions of **4a**−**c** are stable at room temperature in a variety of solvents for several days. Similarly, when **4a**−**c** were heated in cyclohexene or styrene, we found no evidence of nitrene transfer. One possible reason for the lack of reactivity of **4a**−**c** is the steric limitations imposed by the isopropyl groups of the redox-active ligand. Just as these groups may prevent the addition of a fourth chlorine atom to **3**, they may prevent the approach of substrate to the tantalum−imido functional group. As such, we are pursuing methods to open a vacant coordination site of imido complexes such as **4a**−**c** with various halide abstraction reagents.

The formation of diphenylmethylidenehydrazido complex **5** is unusual. To the best of our knowledge, terminal diphenylmethylidenehydrazido−tantalum complexes are unknown, though there are several examples of transition-metal diphenylmethylidenehydrazido complexes[2h,45] and even a uranium−imido−diphenylmethylidenehydrazido complex.[46] Complex **5** compares most closely to $Cp_2NbH(=NNCPh_2)$,[47] which has a similar metal radius; however, the Ph_2CN_2 ligand in the niobium case is much less activated or reduced, as evidenced by a longer Nb=N bond of 1.85 Å and a shorter N−N bond of 1.31 Å. Resonance structure E, and to a lesser extent D, of Scheme 3 are most consistent with the metrical data for the crystal structure

(41) (a) Luetkens, M. L.; Elcesser, W. L.; Huffman, J. C.; Sattelberger, A. P. *Inorg. Chem.* **1984**, *23*, 1718–1726. (b) Labauze, G.; Samuel, E.; Livage, J. *Inorg. Chem.* **1980**, *19*, 1384–1386.
(42) Noh, W.; Girolami, G. S. *Inorg. Chem.* **2008**, *47*, 535–542.
(43) (a) Proulx, G.; Bergman, R. G. *Organometallics* **1996**, *15*, 684–692. (b) Proulx, G.; Bergman, R. G. *J. Am. Chem. Soc.* **1995**, *117*, 6382–6383.
(44) (a) Burckhardt, U.; Casty, G. L.; Gavenonis, J.; Tilley, T. D. *Organometallics* **2002**, *21*, 3108–3122. (b) Schmidt, J. A. R.; Arnold, J. *Organometallics* **2002**, *21*, 3426–3433. (c) Pugh, S. M.; Trösch, D. J. M.; Skinner, M. E. G.; Gade, L. H.; Mountford, P. *Organometallics* **2001**, *20*, 3531–3542. (d) Nielson, A. J.; Glenny, M. W.; Rickard, C. E. F.; Waters, J. M. *J. Chem. Soc., Dalton Trans.* **2000**, 4569–4578.
(45) (a) Hillhouse, G. L.; Haymore, B. L. *J. Am. Chem. Soc.* **1982**, *104*, 1537–1548. (b) Kool, L. B.; Rausch, M. D.; Alt, H. G.; Herberhold, M.; Hill, A. F.; Thewalt, U.; Wolf, B. *Chem. Commun.* **1986**, 408–409. (c) Gerlach, C. P.; Arnold, J. *Organometallics* **1997**, *16*, 5148–5157. (d) Radius, U.; Attner, J. *Inorg. Chem.* **2004**, *43*, 8587–8599. (e) Sydora, O. L.; Kuiper, D. S.; Wolczanski, P. T.; Lobkovsky, E. B.; Dinescu, A.; Cundari, T. R. *Inorg. Chem.* **2006**, *45*, 2008–2021.
(46) Kiplinger, J. L.; Morris, D. E.; Scott, B. L.; Burns, C. J. *Chem. Comm.* **2002**, 30–31.
(47) Nikonov, G. I.; Putala, M.; Zinin, A. I.; Kazennova, N. B.; Lemenovskii, D. A.; Batsanov, A. S.; Struchkov, Y. T. *J. Organomet. Chem.* **1993**, *452*, 87–90.

Scheme 3

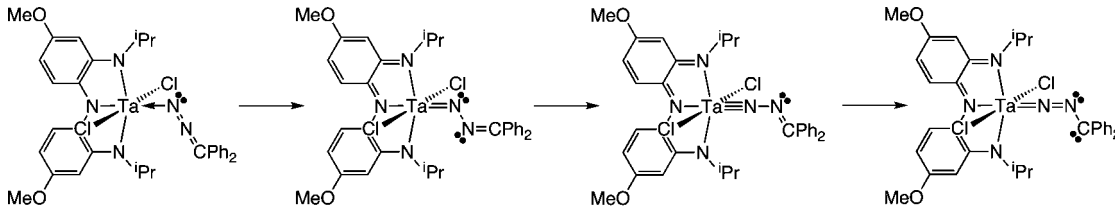

of **5** and provide the best description of the bonding in the diphenylmethylidenehydrazido complex.

Concluding Remarks. The $[NNN^{cat}]^{3-}$ ligand offers a versatile redox-active platform for the synthesis of new tantalum(V) complexes. Superficially this ligand platform resembles the well-known $[ONO^{cat}]^{3-}$ ligand platform that has been exploited extensively, yet three factors distinguish $[NNN^{cat}]^{3-}$. First, the three amides of $[NNN^{cat}]^{3-}$ act as very strong π-donors toward the metal center, effectively making the ligand a 10- or 12-electron donor. Second, the isopropyl groups on the $[NNN^{cat}]^{3-}$ ligand provide a mechanism for steric control at the metal center that is not possible with the $[ONO^{cat}]^{3-}$ ligand. Finally, the $[NNN^{cat}]^{3-}$ ligand presented here has an electron-donating methoxy group in resonance with the amide donors. The synthetic strategy used to prepare the ligand backbone should make it possible to substitute neutral or even electron-withdrawing groups into this position to subtly tune the redox properties of the ligand.

The most important feature of the $[NNN^{cat}]^{3-}$ ligand platform is its ability to enable both one- and two-electron oxidations to the formally tantalum(V) metal center. The nitrene transfer from an organic azide to tantalum(V) complex **1** is particularly novel because it is the first example of a two-electron group transfer reaction that relies exclusively on valence electrons formally associated with the ligand. On the other hand, IR studies of the isonitrile adduct **2** and EPR studies of the one-electron oxidized species **3** indicate that these ligand valence electrons are significantly delocalized onto the metal center. It is likely this mixing of ligand and metal orbitals allows the two-electron group-transfer reaction to proceed moothly.

Acknowledgment. The authors thank Prof. Andy Borovik and Kwanyi "Gary" Ng for assistance with the collection of EPR spectra and Dr. Joe Ziller for assistance with analysis of X-ray diffraction data. NSF-CAREER (CHE-0645685) and the UCI Undergraduate Research Opportunities Program (to AIN) supported this work. A.F.H. is an Alfred P. Sloan Foundation Fellow.

Supporting Information Available: X-ray diffraction data (in CIF format) for **1**, **4a**, and **5**. This material is available free of charge via the Internet at http://pubs.acs.org.

JA808542J